HHS Public Access

Author manuscript

Ophthalmology. Author manuscript; available in PMC 2023 December 01.

Published in final edited form as:

Ophthalmology. 2022 December ; 129(12): 1402–1411. doi:10.1016/j.ophtha.2022.07.001.

Machine-identified Patterns of Visual Field Loss and An Association with Rapid Progression in the Ocular Hypertension Treatment Study

Siamak Yousefi, PhD[1,2], **Louis R. Pasquale, MD**[3], **Michael V. Boland, MD, PhD**[4], **Chris A. Johnson, PhD**[5]

[1]Department of Ophthalmology, University of Tennessee Health Science Center, Memphis, TN

[2]Department of Genetics, Genomics, and Informatics, University of Tennessee Health Science Center, Memphis, TN

[3]Department of Ophthalmology, Icahn School of Medicine at Mount Sinai, New York, USA

[4]Department of Ophthalmology, Massachusetts Eye and Ear, Boston, USA

[5]Department of Ophthalmology and Visual Sciences, University of Iowa Hospitals and Clinics, Iowa City, IA

Abstract

Purpose: To identify patterns of visual field (VF) loss based on unsupervised machine learning and to identify patterns that are associated with rapid progression.

Design: Cross-sectional and longitudinal study.

Participants: A total of 2231 abnormal VFs from 205 eyes of 176 OHTS participants followed over approximately 16 years.

Methods: VFs were assessed by an unsupervised deep archetypal analysis algorithm as well as an OHTS certified VF reader to identify prevalent patterns of VF loss. Machine-identified patterns of glaucoma damage were compared against those patterns previously identified (expert-identified) in the OHTS in 2003. Based on the longitudinal VFs of each eye, VF loss patterns that were strongly associated with rapid glaucoma progression were identified.

Main Outcome Measures: Machine-expert correspondence and type of patterns of VF loss associated with rapid progression.

Results: The average VF mean deviation (MD) at conversion to glaucoma was −2.7 dB (Standard Deviation (SD) = 2.4 dB) while the average MD of the eyes at the last visit was −5.2 dB (SD = 5.5 dB). Fifty out of 205 eyes had MD rate of −1 dB/year or worse and were considered rapid progressors. Eighteen machine-identified patterns of VF loss were compared

Corresponding Author: Siamak Yousefi, 930 Madison Ave., Suite 726, Memphis, TN 38163, Phone: 9014487831, siamak.yousefi@uthsc.edu.

with expert-identified patterns in which 13 patterns of VF loss were similar. The most prevalent expert-identified patterns included partial arcuate, paracentral, and nasal step defects, and the most prevalent machine-identified patterns included temporal wedge, partial arcuate, nasal step, and paracentral VF defects. One of the machine-identified patterns of VF loss predicted future rapid VF progression after adjustment for age, sex, and initial MD.

Conclusions: An automated machine learning system can identify patterns of VF loss and could provide objective, and reproducible nomenclature for characterizing early signs of visual defects and rapid progression in patients with glaucoma.

Precis:

We developed an artificial intelligence system that can discover and classify patterns of visual field loss. Some patterns of visual field loss that were previously unknown predicted future rapid glaucoma progression.

Introduction

Glaucoma is a heterogeneous group of disorders that represents the second leading cause of blindness overall, affecting up to 91 million individuals worldwide.[1,2] Glaucoma has multiple known risk factors including age, ethnicity, and elevated intraocular pressure (IOP).[3,4] However, subjects with one or more of these risk factors may or may not develop glaucoma, making an accurate disease prediction challenging.[5] Since glaucoma is typically asymptomatic, its detection before significant vision loss is critical.[6] Hence, methods for detecting glaucoma at earlier stages could have a significant impact on public health.

Visual field (VF) testing through standard automated perimetry (SAP) remains a clinical standard for glaucoma assessment. Classification of glaucomatous VF defects is important for several reasons: to diagnose the disease through the determination of the pattern and shape of the defect, to identify the severity of disease, to adjust the therapy based on the type of defect and quality of the life, and to determine prognosis.[7] However, manual classification of VFs requires significant clinical training, is subjective with limited reader agreement (even among glaucoma specialists), and more importantly, is labor intensive.[8,9]

Several groups have proposed systems for classifying the severity and pattern of glaucomatous VF loss, which are mostly developed using cross-sectional VF data.[10–13] Other investigators have also developed staging systems as a means of classifying VF progression.[7] An important component of managing patients with glaucoma includes determination of whether changes in the pattern and shape of VF loss indicates disease progression, which may require modification of current therapeutic interventions.

With recent advances in artificial intelligence models and significant growth in data availability, these methods have shown promise for providing objective systems to assess VF data.[14–19] Unlike most machine-learning models that require large, clinically annotated training datasets to learn promising features, we use unsupervised learning requiring no annotated data. The unsupervised machine independently identifies abnormal VF patterns with characteristics of potential interest for predicting visual loss.[17,20–22] Due to their unsupervised nature, these types of learning algorithms are more useful over algorithms that

use predefined assumptions and rules to build knowledge. Moreover, the learning process is more accessible since there is no requirement for human training expertise. Nevertheless, it is desirable to eventually validate these models with input from human experts to assure findings are clinically relevant for an effective utility.

The ability to classify patterns of VF loss is important but anticipating progression before it leads to substantial vision loss (i.e., forecasting rapid progression), is even more crucial to understanding glaucoma, targeting treatment, and preventing vision-related disability. While several risk factors including older age, elevated IOP, African ethnicity, and increased cup-disk ratio may contribute to glaucoma onset and progression [23], we propose an objective approach based on machine-identified patterns of VF loss to predict those who may experience rapid glaucoma progression and future vision loss.

Method

Subjects and Data

Appropriate data use agreements were signed to utilize the de-identified data from the Ocular Hypertension Treatment Study (OHTS). The study was conducted according to the tenets of Helsinki. The OHTS was a prospective, multi-center investigation (22 centers across the US) that sought to prevent or delay the onset of VF loss in patients with elevated IOP (at moderate risk of developing glaucoma). All risk factors were measured at baseline prior to disease onset and clinical data were collected for approximately 16 years (phases 1 and 2 from 1994 to 2008). Clinical examination data and fundus photographs were collected every six months over the course of the study. Details of the OHTS study and the procedures for identifying glaucoma have been described previosuly.[24]

Briefly, VFs were initially collected using the Humphrey Field Analyzer (Carl Zeiss Meditec, Dublin, California) 30–2 pattern, full threshold or SITA Standard strategy, white-on-white perimetry. Two VF tests had to meet reliability criteria of <33% false positives and false negative, and <33% fixation loss errors, be classified as normal by three readers of the OHTS Visual Field Reading Center (VFRC) (including C.A.J), and exhibit a Corrected Pattern Standard Deviation (CPSD) within the 95% age specific population norm, as well as a Glaucoma Hemifield Test (GHT) result within the 97% age-specific population norm (“within normal limits”).

Visual fields had to be normal and reliable in both eyes on two consecutive assessments as determined by the VFRC, and the optic nerves had to be normal in both eyes on clinical examination and in stereoscopic optic disc photographs as determined by the OHTS Optic Disc Reading Center (ODRC). If one of the two baseline VFs were not reliable or consistent with the other VF, a third test was requested by the VFRC. Follow-up VF assessments were performed at 6-month intervals. Due to VF variability, three reliable and reproducible abnormal VFs were required to meet the abnormality criteria for an OHTS VF endpoint. However, at the time of conversion to glaucoma, only one dependable VF was available for each eye in the OHTS dataset. A total of 2,231 VFs corresponding to the onset date of a glaucomatous VF endpoint (assigned based on VF abnormality) as well as the respective

follow-up visits (VFs corresponding to visits after glaucoma onset) were included in this study (one VF per visit).

Unsupervised machine learning model: Archetypal analysis[25] is basically a matrix factorization method where a dataset (matrix) is decomposed as archetypes that lie on (or adjacent to) convex hull (enclosing shape) of input data points. Therefore, archetypes present a convenient method to capture extreme properties of a large number of VFs. Deep archetypal analysis[26–30] is a layered framework that performs multiple archetypal analysis-based factorizations on the input data (matrix) and its subsequent factors. Deep archetypal analysis systematically divides the input data into small groups, thus capturing both local and global characteristics of the data. We loaded the 2,231 abnormal VFs from 176 OHTS participants into a deep archetypal analysis algorithm to identify deep VF archetypes that could be of interest in characterizing VF loss. The deep archetypal analysis identified underlying patterns without supervision or any additional clinical parameter as input. The only parameter that we provided to the DAA algorithm was the number of patterns we expected to identify. We examined different numbers of archetypes and observed that 18 patterns generated the minimum reconstruction error (the root mean square error of initial and reconstructed VFs were assessed objectively and the number of archetypes corresponding to minimum error was selected as the optimal number) as well as providing a mutually exclusive set of patterns (evaluated subjectively by C.A.J). We refer to these 18 patterns as machine-identified patterns of VF loss (Fig. 1) and refer to those patterns that were identified in the initial OHTS study as expert-identified patterns of VF loss (Fig. 2).

Each VF can be represented as a weighted combination of these 18 machine-identified patterns of VF loss while this is not necessarily true for expert-identified patterns of VF loss. To compare machine- and expert-identified patterns of VF loss, we obtained the mutually exclusive patterns of VF loss identified by OHTS certified VF readers (Fig. 2).[13] Next, one of the three OHTS certified VF readers (C.A.J.) was asked to identify the correspondence between these 18 machine-identified patterns with those originally identified in the 2003 OHTS VF classification study.[13] We added another classification, called “other”, in case any of these machine-identified patterns of VF loss did not correspond to any of the original OHTS classifications. We then computed the agreement between the reader and the machine and assessed which patterns were present in both machine-identified and expert-identified groups and which patterns were missing.

To investigate the most prevalent pattern of VF loss among the 18 machine-identified patterns, we decomposed each VF to these 18 machine-identified deep archetypal patterns. We then established a correspondence between each VF and the most contributing machine-identified pattern based on the largest weight (other machine-identified patterns may have non-zero weights). VFs were subsequently clustered to 18 groups corresponding to 18 machine-identified patterns based on largest weight of each VF. To identify the extent and severity of glaucoma in eyes in each cluster, we computed the average Mean Deviation (MD) of eyes in that cluster.

To investigate the association between machine-identified patterns of VF loss and rapid progression, we assessed if the machine-identified patterns of VF loss corresponding to only

the first visit of the sequence of VFs of each eye can predict rapid VF progression. To account for variation in MD of different visits, for each eye, the MD rate was calculated based on the linear regression of MD at all visits and recording the slopes. Eyes with rapid VF progression had MD rate of −1 dB/year or worse. We used generalized estimating equations (GEE) [31] to identify associations to account for both eyes of same subjects.

Results

A total of 205 eyes (of 3,272 eyes) from 176 subjects (of 1,636 participants) in the OHTS were determined to reach a glaucomatous VF endpoint. The average MD from the 205 VFs at the time of conversion (glaucoma onset) was −2.7 dB (±2.4; SD) while the average MD of the eyes at the last visit was −5.2 dB (±5.5). The average MD of all 2,231 longitudinal VFs was −4.2 dB (±4.7).

A total of 50 out of 205 eyes had MD rate of −1 dB/year or worse with mean rate of MD decline of −1.9 dB/year (SD=±1.4, quantiles= [−10.3, −2.1, −1.6, −1.3, −1.0]) and were considered rapid progressors. Eyes that were not progressing rapidly had a mean rate of MD decline of 0.2 dB/year (SD= ±2.1, quantiles= [−1.0, −0.32, −0.11, 0.14, 21.4]).

Figure 1 shows 18 machine identified patterns of VF loss that were prevalent in the VFs of the OHYS study. Figure 2 presents 18 expert-identified patterns of VF loss that were recognized by the OHTS team from the same subset of VFs previously.

Table 1 shows the correspondence between machine- and expert-identified patterns of VF loss as reviewed by one of the OHTS certified VF readers (C.A.J). Patterns without correspondence were labeled as *other.* The OHTS certified VF reader agreed that deep VF archetype P1 is normal, thus there was no correspondence for this archetype among expert-identified patterns of defect.

Machine-identified archetypes P2, P1, P4, and P10 were the most prevalent patterns in the VFs of OHTS participants at the glaucoma conversion visit with 21%, 17%, 10%, and 8%, contributions, respectively (based on analysis of the predominant pattern). The contributions of the remaining patterns were less than 5% across all VFs. Machine-identified archetype P2 was identified as a temporal wedge defect, which was also prevalent in the OHTS initial study. Table 2 shows all patterns and a brief, corresponding explanation based on the initial OHTS study.

Figure 3 shows the box plot of the MD values of clusters of VFs with predominant machine-identified patterns of VF loss. Eyes in which the P1 pattern was predominant (P1 had the highest weight among all 18 DAA patterns) had the least global severity as expected, since this pattern was normal, while eyes with P18 as the predominant pattern had the deepest global severity.

We calculated MD rates of all eyes using the slopes of linear regression models based on the VF test corresponding to the glaucoma conversion date and follow up VFs. We then decomposed the VFs of all eyes corresponding to the glaucoma conversion date only (visits that each eye converted to glaucoma based on the VF endpoint). While P15 pattern was

present in 52% of the VFs of fast progressing eyes, P15 was present in only 9% of the non-progressing eyes (we considered P15 is present if its weight was greater than 1% no matter if P15 is predominant or not).

Machine-identified pattern P15 at the time of glaucoma conversion predicted those with future rapid MD progression. In the GEE model, once we used P15 as the only independent variable to predict rapid progression, estimate, standard error, Wald, and p value were 14.8, 4.3, 11.6, and 0.0006, respectively. When we entered the other machine-identified patterns, initial MD (at the glaucoma onset visit), sex, and age in the GEE equation (accounted for covariates), still the only significant factor that predicted rapid glaucoma progression was P15 (estimate, standard error, Wald, and p value were 15.3, 5.9, 6.8, and 0.009, respectively). In fact, P15 pattern was present in 52% of the VFs of fast progressing eyes, however P15 was present in only 9% of the non-progressing eyes.

Figure 4 shows VFs collected from three OHTS participants at the time of conversion to glaucoma (based on VF endpoint). The VFs were decomposed to 18 deep archetypes based on the proposed unsupervised machine learning technique. The upper panel shows the VF of the left eye of a 60-year-old patient with initial MD of 1.2 dB that the weight of its P15 pattern was 0%. The rate of MD progression of this subject was −0.32 dB/year, and the subject was a non-rapid progressor. The middle panel represents the VF of the left eye of a 40-year-old patient with initial MD of −6.8 dB in which the weight of its P15 pattern was 0%. The rate of MD progression of this subject was 0.50 dB/year thus a non-rapid progressor. The lower panel represents the VF of the right eye of a 75-year-old patient with initial MD of −6.7 dB in which the weight of its P15 pattern was 16%. The rate of MD progression of this subject was −2.46 dB/year so was progressing rapidly.

Discussion

We observed that for 13 of the machine-identified patterns of VF loss, there is a general agreement between a certified VF grader on the corresponding expert-determined patterns.

Except for P11 which was identified as quadrantanopia, there was no pattern reflecting a neurological defect based on the machine-identified patterns of VF loss. However, OHTS readers had identified homonymous patterns of VF loss in the OHTS dataset. The algorithm identified patterns of VF loss (see Table 1: P3, P14, and P15) that were not recognized in the OHTS classification study. There was a tendency towards macular and foveal loss in machine-identified patterns of VF loss. For instance, pattern P3 likely corresponds to VF defects in the macula and fovea regions. Patterns P14, P15, and P17 that were absent in the OHTS study but present in our model partially included macular and corneal regions. Both the machine-identified (Fig. 3) and the expert-identified[13] temporal wedge pattern of VF loss had a relatively small MD compared to other patterns of VF loss. Also, both studies identified that the total loss pattern has the deepest MD.

While the experts in the initial OHTS study identified only one class for partial arcuate patterns of VF loss, the algorithm discovered four subtypes of partial arcuate patterns of VF loss (P4, P10, and P12). P4 was of particular note as the arcuate in the inferior region of the

VF was not highlighted in the initial OHTS study, but this rare pattern was discovered by machine learning.

There may be several reasons for the discrepancy between machine-identified and expert-identified patterns of VF loss, one of which could be the process that was followed to identify such patterns manually. OHTS readers limited the findings to a single prominent pattern for each VF and did not classify more complicated patterns that were likely a combination of multiple simpler patterns. However, the machine algorithm does not exclude any pattern and tries to decompose more complex VFs to those 18 deep archetypes and then select one with highest weight as the prominent pattern.

We derived patterns of VFs of all eyes at the glaucoma conversion visit in which the average MD across all eyes was only −2.7 dB. Therefore, it is expected that the predominant patterns mostly include P1 to P4. In fact, P1, P2, and P4 contributed to approximately 50% of the weight across all VFs (17%, 21%, and 10%, respectively). The other patterns contributed about 5% or less. The difference between the weights of the P15 pattern in non-rapid and rapid progressors was statistically significant (based on GEE test accounting for both eyes of subjects, age, and initial MD). Visual field testing is the most common method to assess glaucoma progression in clinical practice. It also reflects functional vision loss which likely has a more direct impact on patient quality of life. As such, the weight of P15 pattern (which was not recognized in the initial OHTS study) could be used to predict future rapid glaucoma progression.

Overall, computer algorithms are more consistent compared to groups of glaucoma specialists and well-trained readers in making subjective judgements concerning VF patterns and shapes. While human experts may not follow the guidelines and procedures precisely[32], computer algorithms consistently follow such guidelines and procedures and can reproduce the same results from the same corresponding guidelines. Computers can produce algorithms at a much faster and more consistent, uninterrupted pace compared to practitioners faced with other clinical duties. Machine algorithms may help us move beyond the limitations of human cognition if they can identify hidden patterns corresponding to preclinical and early stages of the disease process.

While computer algorithms are inherently objective, human experts are more likely to be subjective regardless of how we specify procedures and blind them to records. The computer algorithms we developed did not take into account any other clinical characteristics of OHTS patients except for the VF. Although OHTS VF graders did not have access to any other information when they categorized patterns, they did have a background and experience in recognizing VF loss patterns consistent with glaucoma and also patterns that are not consistent with glaucoma (e.g., retinal and neurologic disorders). Such background information and experience can be an advantage, but it eventually introduces sources of bias leading to assessments that are not completely objective.

The present investigation has some limitations: (1) All the OHTS patients had reliable and consistent normal VFs and optic discs when they entered the study at baseline. The ensuing VF loss therefore represents early deficits and may not be representative of more

advanced glaucomatous functional deficits. (2) Another limitation is that findings may not be broadly applicable to all glaucoma patients as our findings were derived from patients with elevated IOP, open angles and no evidence of secondary cause for glaucoma. (3) The current investigation was directed towards recognizing patterns and shapes of baseline (at the onset date) VF loss associated with rapid glaucomatous progression, but not longitudinal changes in VF characteristics that would be associated with glaucomatous progression. (4) The correspondence analysis between the ML VF patterns and the expert-derived patterns was inherently qualitative and somewhat subjective but conducted by an OHTS VFRC expert. (5) Findings may not be broadly applicable to all glaucoma patients as our study just investigated ocular hypertensive patients with open angles and no evidence of secondary cause for glaucoma. (6) Additional computational power is required to be able to perform the AA determinations. (7) To be useful in a busy clinical setting and for this algorithm to be readily and rapidly accessible to practitioners, this system would have to be integrated into clinical systems which would require system development and regulatory approval.

In summary, the current study indicates that deep archetypal analysis of VF results can be used to identify patterns and shapes of functional loss. Moreover, one pattern was found to be predictive of future rapid progression. With further refinements of this process and implementation of larger glaucomatous datasets displaying representing a wide range of severity and combined with longitudinal assessment, this procedure could become a valuable and useful tool for practitioners who manage glaucoma patients.

Conclusion

We have developed an AI system that can identify prevalent patterns of VF loss without human intervention. While expert classification of VF loss is labor-intensive with poor agreement among experts, machine learning algorithm can discover and classify patterns of VF loss quickly in a consistent manner. This new AI system can aid glaucoma specialists in identifying patterns of VF loss objectively and may aid in identifying those patients at higher risk of developing particular types of VF loss that may impact their daily activity and quality of living.

Acknowledgment

This work was supported by NIH Grants EY033005 (SY), EY030142 (SY), R21EY031725 (SY), Challenge Grant from Research to Prevent Blindness (SY), and R01EY015473 (LRP). The funders had no role in study design, data collection and analysis, decision to publish, or preparation of the manuscript. LRP is also supported by Research to Prevent Blindness (NYC) and The Glaucoma Foundation (NYC).

References

1. Quigley HA. Number of people with glaucoma worldwide. Br J Ophthalmol. 1996;80(5):389–393. [PubMed: 8695555]
2. Goldberg I.How common is glaucoma worldwide? In: Weinreb RN, Kitazawa Y, Krieglstein GK, eds. Glaucoma in the 21st Century. London: Mosby International; 2000:3–8.
3. Leske MC, Connell AM, Wu SY, Hyman LG, Schachat AP. Risk factors for open-angle glaucoma. The Barbados Eye Study. Arch Ophthalmol. 1995;113(7):918–924. [PubMed: 7605285]
4. Coleman AL, Miglior S. Risk factors for glaucoma onset and progression. Surv Ophthalmol. 2008;53 Suppl1:S3–10. [PubMed: 19038621]

5. Jiang X, Varma R, Wu S, et al. Baseline risk factors that predict the development of open-angle glaucoma in a population: the Los Angeles Latino Eye Study. Ophthalmology. 2012;119(11):2245–2253. [PubMed: 22796305]
6. Johnson DH. Progress in glaucoma: early detection, new treatments, less blindness. Ophthalmology. 2003;110(4):634–635. [PubMed: 12689878]
7. Brusini P, Johnson CA. Staging functional damage in glaucoma: review of different classification methods. Surv Ophthalmol. 2007;52(2):156–179. [PubMed: 17355855]
8. Lichter PR. Variability of expert observers in evaluating the optic disc. Trans Am Ophthalmol Soc. 1976;74:532–572. [PubMed: 867638]
9. Jampel HD, Friedman D, Quigley H, et al. Agreement among glaucoma specialists in assessing progressive disc changes from photographs in open-angle glaucoma patients. Am J Ophthalmol. 2009;147(1):39–44 e31. [PubMed: 18790472]
10. Brusini P.Clinical use of a new method for visual field damage classification in glaucoma. Eur J Ophthalmol. 1996;6(4):402–407. [PubMed: 8997583]
11. Henson DB, Spenceley SE, Bull DR. Spatial classification of glaucomatous visual field loss. Br J Ophthalmol. 1996;80(6):526–531. [PubMed: 8759263]
12. Anton A, Maquet JA, Mayo A, Tapia J, Pastor JC. Value of logistic discriminant analysis for interpreting initial visual field defects. Ophthalmology. 1997;104(3):525–531. [PubMed: 9082284]
13. Keltner JL, Johnson CA, Cello KE, et al. Classification of visual field abnormalities in the ocular hypertension treatment study. Arch Ophthalmol. 2003;121(5):643–650. [PubMed: 12742841]
14. Bowd C, Weinreb RN, Balasubramanian M, et al. Glaucomatous patterns in Frequency Doubling Technology (FDT) perimetry data identified by unsupervised machine learning classifiers. PLoS One. 2014;9(1):e85941.
15. YousefS, GoldbauH, BalasubramaniaM, et al. . Learning from data: recognizing glaucomatous defect patterns and detecting progression from visual field measurements. IEEE Trans Biomed Eng. 2014;61(7):2112–2124. [PubMed: 24710816]
16. Yousefi S, Goldbaum MH, Zangwill LM, Medeiros FA, Bowd C. Recognizing patterns of visual field loss using unsupervised machine learning. Proc SPIE Int Soc Opt Eng. 2014;2014.
17. Yousefi S, Balasubramanian M, Goldbaum MH, et al. Unsupervised Gaussian Mixture-Model With Expectation Maximization for Detecting Glaucomatous Progression in Standard Automated Perimetry Visual Fields. Transl Vis Sci Technol. 2016;5(3):2.
18. Elze T, Pasquale LR, Shen LQ, Chen TC, Wiggs JL, Bex PJ. Patterns of functional vision loss in glaucoma determined with archetypal analysis. J R Soc Interface. 2015;12(103).
19. Wang M, Shen LQ, Pasquale LR, et al. Artificial Intelligence Classification of Central Visual Field Patterns in Glaucoma. Ophthalmology.
20. Yousefi S, Yousefi E, Takahashi H, et al. Keratoconus severity identification using unsupervised machine learning. PLoS One. 2018;13(11):e0205998.
21. Yousefi S, Goldbaum MH, Shahrian EV, et al. Unsupervised machine learning to recognize glaucoma defect patterns and detect progression in RNFL thickness measurements. Investigative Ophthalmology & Visual Science. 2015;56(7):4564–4564.
22. Yousefi S, Elze T, Pasquale LR, Boland M. Glaucoma monitoring using manifold learning and unsupervised clustering. Paper presented at: 2018 International Conference on Image and Vision Computing New Zealand (IVCNZ)2018.
23. Gordon MO, Beiser JA, Brandt JD, et al. The Ocular Hypertension Treatment Study: baseline factors that predict the onset of primary open-angle glaucoma. Arch Ophthalmol. 2002;120(6):714–720; discussion 829–730. [PubMed: 12049575]
24. Gordon MO, Kass MA. The Ocular Hypertension Treatment Study: design and baseline description of the participants. Arch Ophthalmol. 1999;117(5):573–583. [PubMed: 10326953]
25. Cutler A, Breiman L. Archetypal Analysis. Technometrics. 1994;36(4):338–347.
26. Sebastian Mathias Keller MS, Mario Wieser, Volker Roth.Deep Archetypal Analysis. arXiv:190110799v1. Jan 2019.
27. Thakur A, Abrol V, Sharma P, Rajan P. Deep Convex Representations: Feature Representations for Bioacoustics Classification. Paper presented at: INTERSPEECH2018.

28. Thakur A, Rajan P. Deep Archetypal Analysis Based Intermediate Matching Kernel for Bioacoustic Classification. IEEE Journal of Selected Topics in Signal Processing. 2019;13(2):298–309.

29. Gupta K, Thakur A, Goldbaum M, Yousefi S. Glaucoma Precognition: Recognizing Preclinical Visual Functional Signs of Glaucoma. Paper presented at: 2020 IEEE/CVF Conference on Computer Vision and Pattern Recognition Workshops (CVPRW); 14–19 June 2020, 2020.

30. Thakur A, Goldbaum M, Yousefi S. Convex Representations Using Deep Archetypal Analysis for Predicting Glaucoma. IEEE J Transl Eng Health Med. 2020;8:3800107.

31. Zeger SL, Liang KY, Albert PS. Models for longitudinal data: a generalized estimating equation approach. Biometrics. 1988;44(4):1049–1060. [PubMed: 3233245]

32. O'NeilC, GurriU, PandaS, et al. . Glaucomatous optic neuropathy evaluation project: factors associated with underestimation of glaucoma likelihood. JAMA Ophthalmol. 2014;132(5):560–566. [PubMed: 24699817]

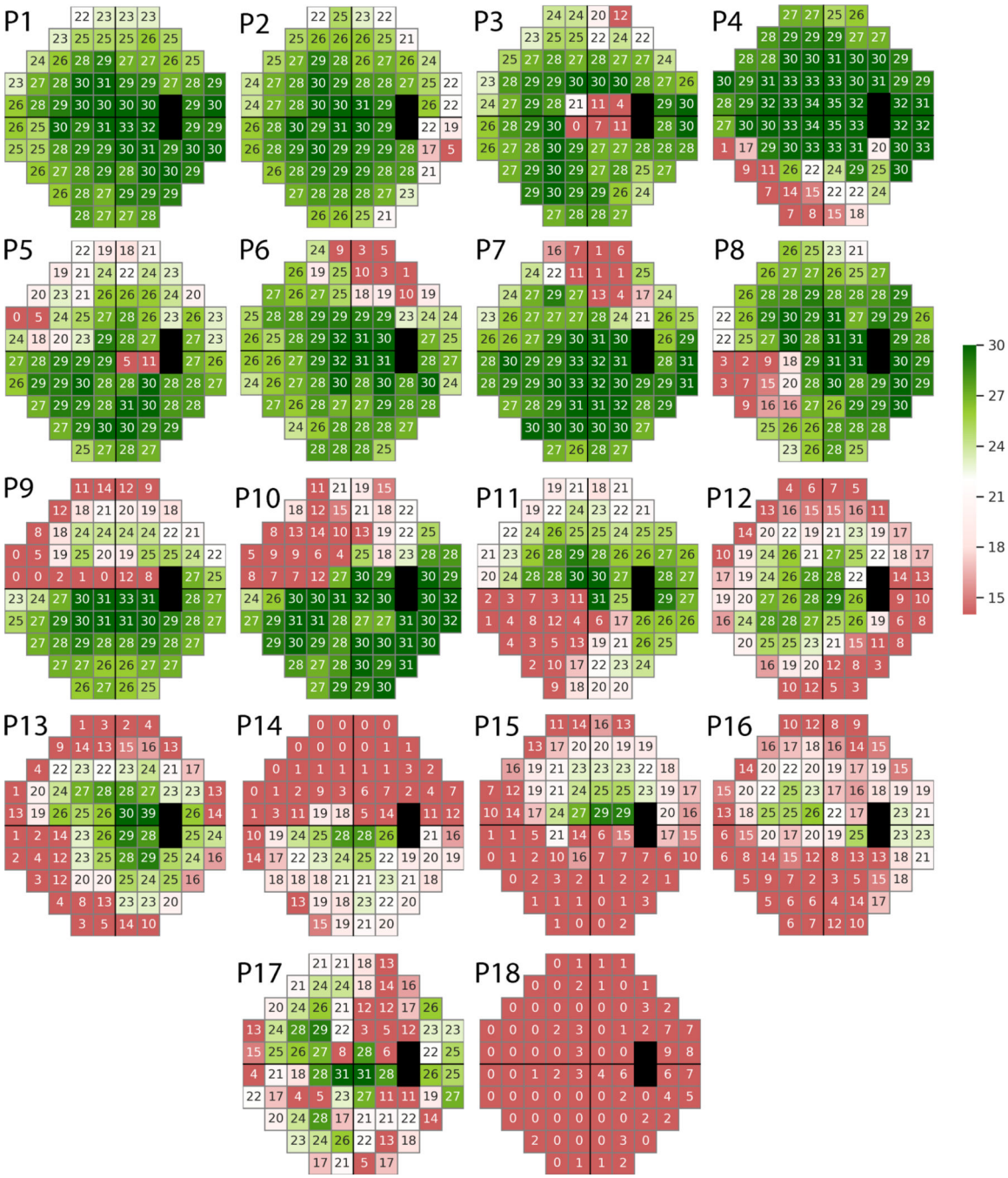

Figure 1.

Deep archetypal analysis (DAA) identified 18 patterns of loss from visual fields of the Ocular Hypertension Treatment Study (OHTS) participants who reached a glaucomatous visual field endpoint in 2003.

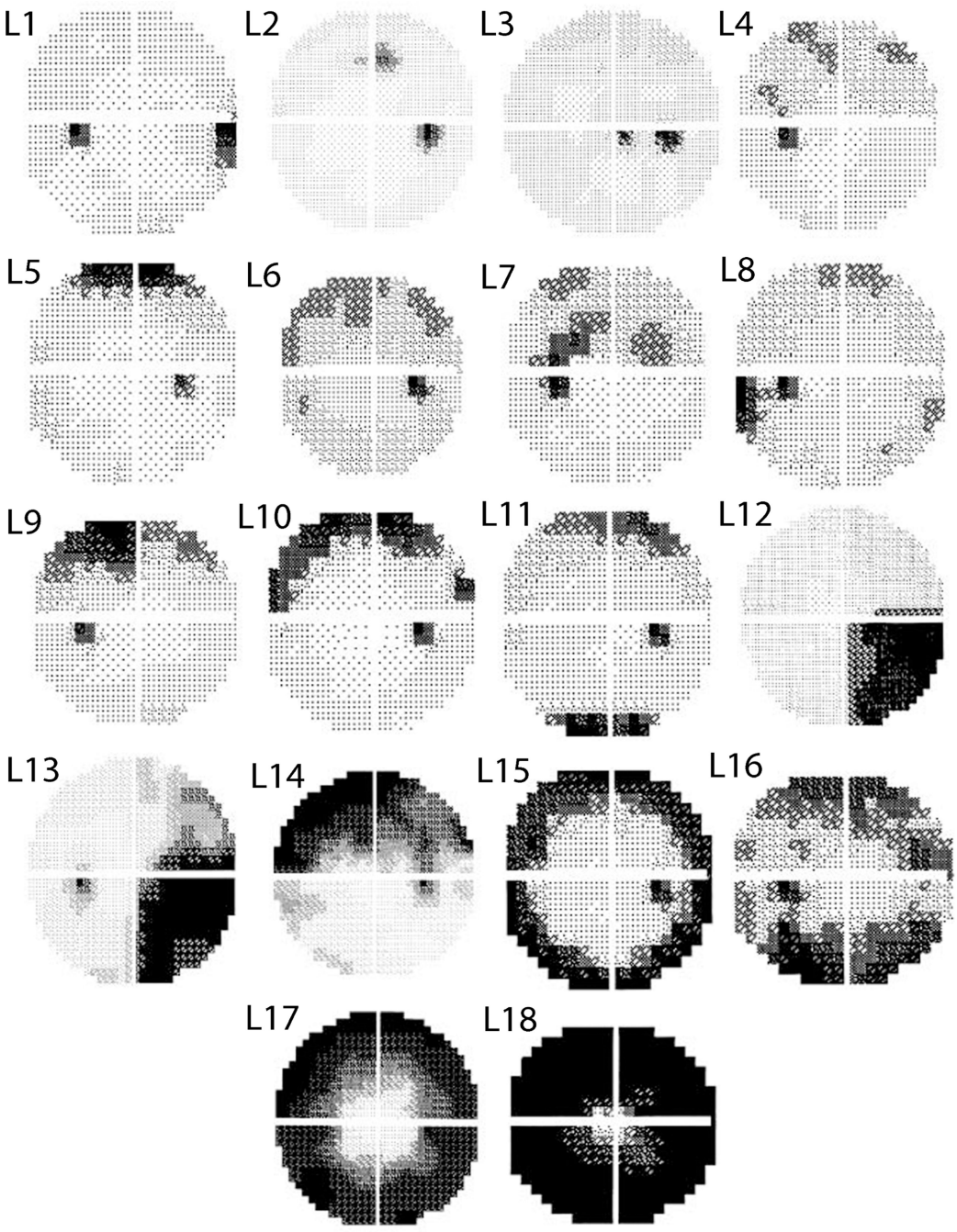

Figure 2.
Three OHTS certified visual field readers identified (mutually exclusive) abnormal visual field patterns denoted in black from the OHTS participants who reached a glaucomatous visual field endpoint in 2003.

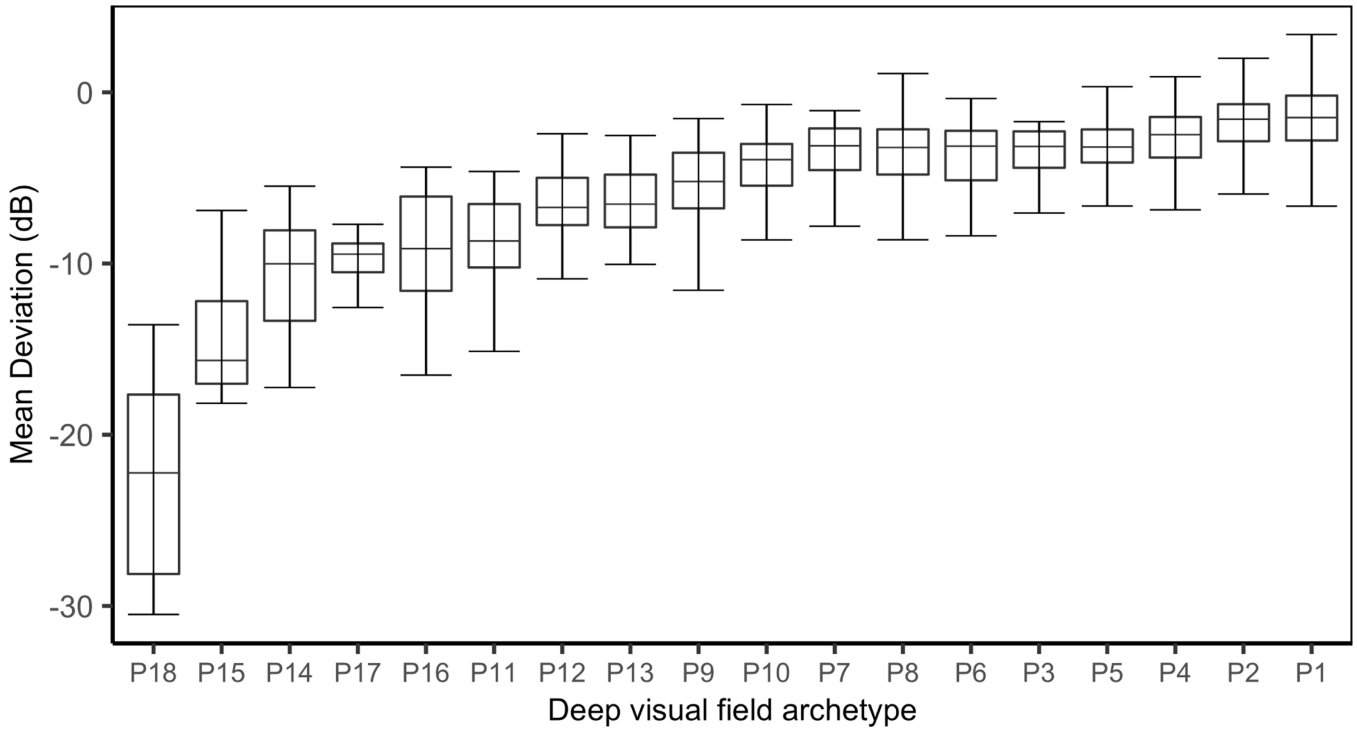

Figure 3.

Boxplot of the visual field mean deviation (MD) values of 18 clusters of visual fields corresponding to machine-identified patterns of visual field loss (archetypes). Eyes with predominant archetype number 1 had the least and eyes with predominant archetype number 18 had the worst average MD.

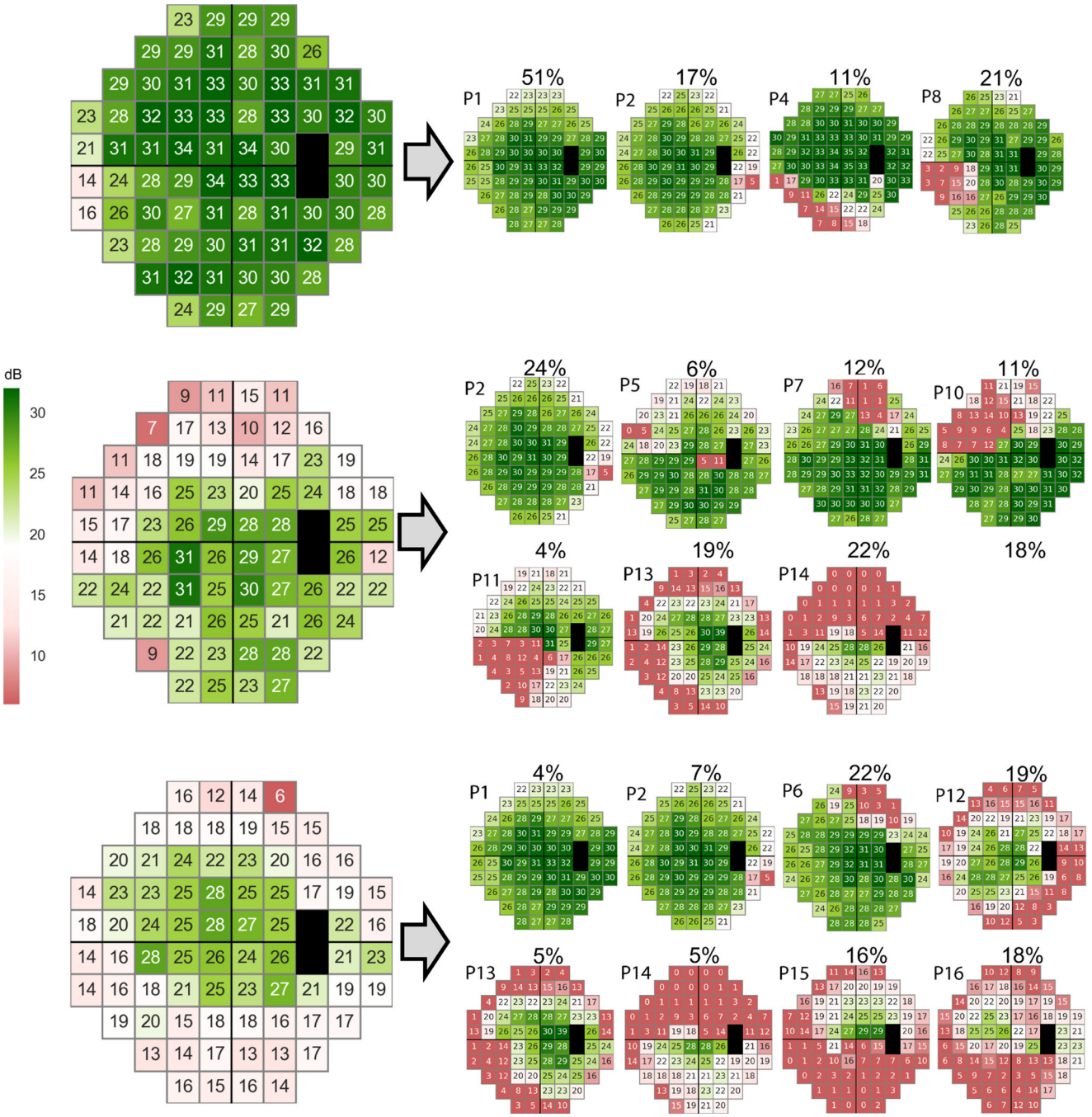

Figure 4.

Three sample abnormal visual fields of eyes with no rapid progression and rapid progression. **Upper**: An abnormal visual field with MD of 1.2 dB (at the time of conversion to glaucoma based on visual field endpoint) was decomposed into 18 deep archetypes in which the weight of the P15 pattern was 0%. This eye did not progress rapidly. **Middle**: An abnormal visual field with MD of −6.8 dB was decomposed into 18 deep archetypes in which the weight of the P15 pattern was 0%. This eye did not progress rapidly. **Lower**: An

abnormal visual field with MD of −6.7 dB was decomposed to deep archetypes in which the weight of the P15 pattern was 16%. This eye progressed rapidly.

Table 1.

Correspondence between machine-identified (based on Fig. 1 labels) and expert-identified (based on labels in Figure 2) patterns of visual field loss by one of the OHTS certified visual field readers.

Machine Identified Pattern (Fig 1)	P1	P2	P3	P4	P5	P6	P7	P8	P9	P10	P11	P12	P13	P14
Expert Identified Pattern (Johnson)	Other	L8	Other	L7	L1	L2	L2	L1	L7	L7	L12	L7	L15	Other
Pattern Name (Johnson)	Normal	Temporal Wedge	Macula	Partial Arcuate	Nasal Step	Paracentral	Paracentral	Nasal Step	Partial Arcuate	Partial Arcuate	Quadrant	Partial Arcuate	Peripheral Rim	Altitu

Table 2.

Category of the machine-identified and expert-identified patterns of visual field loss.

Nerve fiber bundle abnormalities	
Altitudinal (Alt)	Severe visual field loss throughout the entire superior or inferior hemifield that respects the horizontal midline. The entire horizontal midline demonstrates abnormality.
Arcuate (Arc)	Significant visual field loss in the nerve fiber bundle region. Extends across contiguous abnormal points from the blind spot to at least 1 point outside 15° adjacent to the nasal meridian.
Nasal Step (NS)	Limited field loss adjacent to the nasal horizontal meridian. Includes at least 1 abnormal point at or outside 15° on the meridian. Cannot include more than 1 significant point (on either plot) in the nerve fiber bundle region on the temporal side.
Paracentral (Pc)	A relatively small visual field abnormality in the nerve fiber bundle region. Generally, not contiguous with the blind spot or the nasal meridian. Does not involve points outside 15° that are adjacent to the nasal meridian.
Partial Arcuate (PArc)	Visual field loss in the nerve fiber bundle region that extends incompletely from the blind spot to the nasal meridian. The defect is generally contiguous with either the blind spot or the nasal meridian. Must include at least 1 abnormal location in the temporal visual field.
Temporal Wedge (TW)	A small visual field defect that is temporal to the blind spot.
Non-nerve fiber bundle abnormalities	
Central (C)	Visual field loss that is predominantly in the macular region. The foveal threshold must have a P value of less than 0.05. Can be associated with a single hemifield and paired with another defect.
Hemianopia (H)	Hemianopia (H): A visual field defect that respects the vertical meridian. Involves essentially all points in a vertical hemifield.
Inferior Depression (ID)	2 or more abnormal points in the very inferior region.
Partial Hemianopia (PH)	A visual field defect that respects the vertical meridian. Greater than 1 quadrant but less than a complete vertical hemifield.
Partial Peripheral Rim (PPR)	Generally continuous field loss outside 15°. Not in all quadrants. Must have some curvature.
Peripheral Rim (PR)	Generally continuous visual field loss outside 15° in all 4 quadrants. Usually no visual field loss inside 15° on either deviation plot. Must be visual field loss temporal to the blind spot.
Quadrant (Q)	Significant visual field loss throughout an entire quadrant that respects the vertical and horizontal midlines. Essentially all points must have a P value of less than .05 on the total deviation plot.
Superior Depression (SD)	Two or more abnormal points in the very superior region.
Total Loss (TL)	Severe widespread visual field loss (MD <=−20.00 dB).
Vertical Step (VS)	Limited visual field loss that respects the vertical meridian. Includes at least 2 abnormal points at or outside 15° along the vertical meridian.
Widespread (Wsp)	Diffuse visual field loss that includes all 4 quadrants. The glaucoma hemifield test may show a general reduction of sensitivity or the mean deviation must show a P value of less than .05. The corrected pattern SD must not show a P value of less than .05. Most abnormal points on the total deviation plot are not abnormal on the pattern deviation plot.